Harnessing Infrared Photons for Photoelectrochemical Hydrogen Generation. A PbS Quantum Dot Based "Quasi-Artificial Leaf"

ARTICLE *in* JOURNAL OF PHYSICAL CHEMISTRY LETTERS · DECEMBER 2012

Impact Factor: 7.46 · DOI: 10.1021/jz301890m

9 AUTHORS, INCLUDING:

Cornelia Sima
National Institute for Laser, Plasma and Radia…
37 PUBLICATIONS **214** CITATIONS
SEE PROFILE

Iván Mora-Seró
Universitat Jaume I
129 PUBLICATIONS **7,868** CITATIONS
SEE PROFILE

Francisco Fabregat-Santiago
Universitat Jaume I
97 PUBLICATIONS **7,573** CITATIONS
SEE PROFILE

Sixto Giménez
Universitat Jaume I
75 PUBLICATIONS **2,741** CITATIONS
SEE PROFILE

THE JOURNAL OF PHYSICAL CHEMISTRY Letters

Letter

pubs.acs.org/JPCL

Harnessing Infrared Photons for Photoelectrochemical Hydrogen Generation. A PbS Quantum Dot Based "Quasi-Artificial Leaf"

Roberto Trevisan,[†] Pau Rodenas,[†] Victoria Gonzalez-Pedro,[†] Cornelia Sima,[†,‡,§] Rafael S. Sanchez,[†] Eva M. Barea,[†] Ivan Mora-Sero,*[,†] Francisco Fabregat-Santiago,[†] and Sixto Gimenez*[,†]

[†]Photovoltaics and Optoelectronic Devices Group, Departament de Física, Universitat Jaume I, 12071 Castelló, Spain

[‡]National Institute of Lasers, Plasma and Radiation Physics, Atomistilor 409 Street, P.O. Box MG 36 Bucharest-Magurele, 077125 Romania

[§]Faculty of Physics, University of Bucharest, Atomistilor 405 Street, MG-11 Bucharest-Magurele, 077125 Romania

Supporting Information

ABSTRACT: Hydrogen generation by using quantum dot (QD) based heterostructures has emerged as a promising strategy to develop artificial photosynthesis devices. In the present study, we sensitize mesoporous TiO_2 electrodes with in-situ-deposited PbS/CdS QDs, aiming at harvesting light in both the visible and the near-infrared for hydrogen generation. This heterostructure exhibits a remarkable photocurrent of 6 mA·cm^{-2}, leading to 60 mL·cm^{-2}·day^{-1} hydrogen generation. Most importantly, confirmation of the contribution of infrared photons to H_2 generation was provided by the incident-photon-to-current-efficiency (IPCE), and the integrated current was in excellent agreement with that obtained through cyclic voltammetry. The main electronic processes (accumulation, transport, and recombination) were identified by impedance spectroscopy, which appears as a simple and reliable methodology to evaluate the limiting factors of these photoelectrodes. On the basis of this TiO_2/PbS/CdS heterostructrure, a "quasi-artificial leaf" has been developed, which has proven to produce hydrogen under simulated solar illumination at (4.30 ± 0.25) mL·cm^{-2}·day^{-1}.

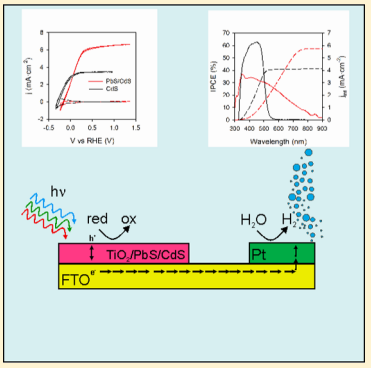

SECTION: Energy Conversion and Storage; Energy and Charge Transport

The provision of clean and renewable energy to satisfy the increasing human demands in the 21st century is one of the key challenges to sustain the present global social and economical model.[1,2] Sunlight offers a huge potential for global supply of renewable energy, provided that this energy can be stored for its use upon demand. In this context, photoelectrochemical hydrogen generation by water splitting with semiconductor materials constitutes the simplest conversion scheme because H_2 can be produced with only the input of water and sunlight, and H_2 combustion in hydrogen fuel cells leads to electricity, with water as the only byproduct, resulting in a CO_2 neutral process.[2−4] The key challenge of this approach relies on whether this goal can be met in a cost-effective way on the terawatt scale.[2]

Since the seminal report of Fujishima and Honda in 1972 demonstrating the photocatalysis of TiO_2 for H_2 generation,[5] a dynamic search for the optimum semiconductor material and device configuration was launched, but crystallization of this research activity into a well-developed technology has not been achieved yet, mainly because none of the explored materials simultaneously meet the different needed requirements for adequate device operation; that is, a band gap comprised between 1.9 and 2.2 eV, conduction and valence band edges straddling the water oxidation and hydrogen reduction potentials, good conductivity, and low cost.[2,4] The novel developments in the fields of nanoscience and catalysis[6] have provided key elements and concepts to rationalize the search for promising materials and device architectures. Orthogonalization of light absorption and carrier diffusion,[7−9] quantum confinement,[10] band energetics engineering,[11] and plasmonics[12,13] appear as fascinating strategies, which can be exploited to enhance the efficiencies of photoelectrochemical hydrogen generation devices. Sensitization of wide band gap oxide semiconductors like ZnO or TiO_2 by chalcogenide quantum dots (QDs) also provides a convenient heterostructured platform for photoelectrochemical H_2 generation. Indeed, this approach has shown promising results. Hensel et al. showed the synergistic effect of N doping of TiO_2 nanowires and CdSe sensitization, leading to photocurrents close to 3 mA·cm^{-2}.[14] Combining ZnO nanowires with CdTe QDs, Chen et al. obtained photocurrents close to 2 mA·cm^{-2} using a nonsacrificial hole scavenger.[15] Hierarchical ZnO/WO_x nanowires co-sensitized with CdSe/CdS led to promising photocurrents close to 12 mA·cm^{-2} and light-to-chemical conversion efficiencies of 6%.[16] More recently, Luo et al. have highlighted the importance of the controlled deposition of the light-

Received: November 19, 2012
Accepted: December 11, 2012
Published: December 11, 2012

absorbing semiconductor (CdSe) on inverse opals of TiO_2, achieving photocurrents of 15.7 mA·cm^{-2} for hydrogen generation.[17]

On the other hand, an optimal exploitation of the solar spectrum for photoelectrochemical energy conversion must entail the use of narrow band gap semiconductors, like PbS, in order to harness infrared photons for photoelectrochemical conversion. Tada et al.[18] have reported a solar-to-hydrogen conversion efficiency of 1.15% and a hydrogen production rate of 5.2 mL·h^{-1} employing a heterostructure based on mesoporous TiO_2 decorated with colloidal PbS QDs (under the application of bias). In the present study, we have developed a hybrid architecture based on a TiO_2 mesoporous frame functionalized with in-situ-grown PbS/CdS QDs, targeting an unassisted photoelectrochemical hydrogen generation device. The ultimate goal is achieving a system able to convert visible but also infrared photons into H_2. Great benefit can be derived from the collection of IR photons because they represent practically 50% of the solar spectrum photons.

We have incorporated in-situ-grown PbS QDs onto a mesoporous TiO_2 structure together with CdS QDs to both enhance the visible response (see Supporting Information Figure SI1) and stabilize the whole material.[19] The microscopic inspection of the material by SEM showed the mesoporous TiO_2 structure but did not reveal any morphological details of the PbS/CdS sensitizers (Supporting Information Figure SI2). The presence of PbS QDs was confirmed through XRD spectra carried out on TiO_2/PbS structures (Supporting Information Figure SI3). High-resolution TEM images (Supporting Information Figure SI4) reveal that both PbS and CdS appear as scattered nanoparticles (diameter below 10 nm) on the mesoporous TiO_2 network and are covered by a ZnS layer.

The photoelectrochemical behavior of TiO_2/PbS/CdS heterostructures in an aqueous solution containing 0.25 M Na_2S and 0.35 M Na_2SO_3 as the sacrificial hole scavenger in the dark and under illumination is shown in Figure 1a. As a

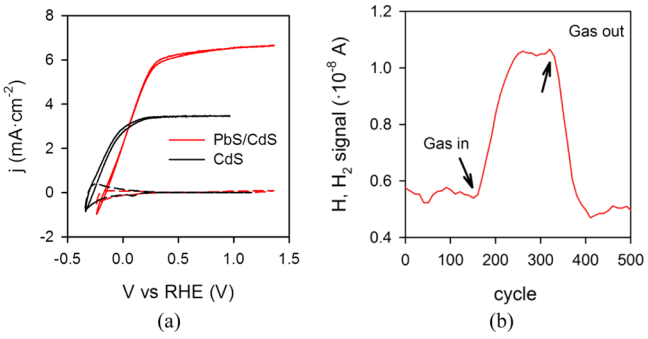

Figure 1. (a) $j-V$ curves for the TiO_2/PbS/CdS heterostructure in the dark (dashed lines) and under illumination at 100 mW·cm^{-2} (solid lines) obtained by cyclic voltammetry in a three-electrode configuration; the results for TiO_2/CdS are also included as a reference. (b) Gas chromatography mass spectroscopy plot of the evolved gas for the TiO_2/PbS/CdS heterostructure. The signal of H_2 is clearly increased after gas is passed through the system.

reference, results for TiO_2/CdS are also included. It is clear that higher photocurrents are obtained when PbS is included in the heterostructures. At 0 V versus RHE, a photocurrent of 2 mA·cm^{-2} is obtained for both systems. Saturation of the photocurrent takes place at approximately 0.4 V versus RHE, with 6 mA·cm^{-2} for TiO_2/PbS/CdS and 3.5 mA·cm^{-2} for TiO_2/CdS. This equals 60 and 35 mL·cm^{-2}·day^{-1} hydrogen generation rates, respectively, assuming a faradaic efficiency of unity. The observed positive photocurrents correspond to hole injection from the heterostructured TiO_2/QDs photoanode into the solution. The difference between the anodic and cathodic branches of the dark cyclic voltammetry curve at potentials below 0 V versus RHE (more visible for the TiO_2/CdS structure) is due to the chemical capacitance of TiO_2, consistent with previous studies.[20−22] Labeling experiments of the evolved gas at the Pt counterelectrode were collected in an inverted buret and analyzed. The results for TiO_2/PbS/CdS are shown in Figure 1b, clearly indicating that the generated gas is hydrogen. Additionally, the stability of these photoelectrodes was tested by chronoamperometric measurements. The electrodes were shown to be stable (no decrease of photocurrent during more than 1 h), and the loss of performance detected was due to the depletion of the sacrificial agent in the solution (see Supporting Information Figure SI5).

The results obtained from the photoelectrochemical characterization shown in Figure 1a suggest that TiO_2, PbS, and CdS form a cascaded structure, and photogenerated electrons at both CdS and PbS can be collected at the contact, although further research is needed to unambiguously establish this point. Figure 2 shows a proposed energy diagram, based on

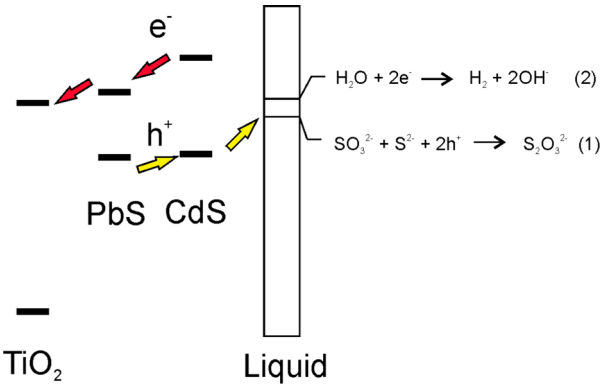

Figure 2. Energy diagram illustrating the oxidation at PbS/CdS QD-sensitized TiO_2 particulate anodes. Energy levels were adapted from refs 25 and 26. The arrows indicate the traffic of electrons and holes.

literature data,[24,25] in which the different electronic processes and relevant electrochemical reactions are scheduled. Further quantification of the position of the energy levels of the conduction and valence band edges for QDs is out of the scope of the present study. Extensive discussion of the reaction mechanisms has been reported elsewhere.[14,15,18,23,24] The presence of Na_2S and Na_2SO_3 hole scavengers in the electrolyte provides a fast shuttle for the photogenerated holes (reaction 1) avoiding photocorrosion while electrons are driven through TiO_2 toward the contact and then to the catalytic cathode, where hydrogen generation takes place (reaction 2).

In order to gain further insight into the charge-transfer mechanisms of TiO_2/PbS/CdS heterostructuctures, chopped light $j-V$ curves were carried out. Figure 3a shows the superimposed chopped and constant light $j-V$ curves. The presence of current transients (spikes) in the chopped light curve provides direct evidence of the participation of surface states in the hole-transfer process. Indeed, the presence of these transients has been attributed to the charging (trapping of holes) of surface states or oxidizing surface species.[27−29] The

dx.doi.org/10.1021/jz301890m | J. Phys. Chem. Lett. 2013, 4, 141−146

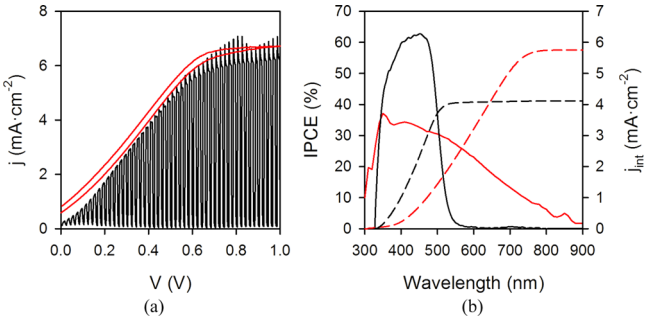

Figure 3. (a) Chopped light (black) and constant (red) illumination $j-V$ curves in two electrode configuration of the TiO_2/PbS/CdS heterostructured photoanode. (b) IPCE (solid lines) and integrated current (dashed lines) for a TiO_2/PbS/CdS (red) and reference TiO_2/CdS (black) photoelectrode at 0.95 V versus RHE.

presence of surface states for PbS has also been recognized in the recombination process for quantum-dot-sensitized solar cells.[19] In contrast, we have previously shown that when CdS/CdSe QDs are used as light absorbers, the hole collection efficiency is unity (spikes are not observed in the chopped light $j-V$ curves).[30]

The contribution of infrared photons to the higher photocurrent measured for TiO_2/PbS/CdS (and hence to the H_2 generation) was assessed by measuring the incident-photon-to-current-efficiency (IPCE) action spectrum in a three-electrode configuration, at 0.95 V versus RHE. The results for TiO_2/CdS are also shown as a reference (see Figure 3b). The IPCE action spectrum for TiO_2/CdS extends up to 550 nm, while when PbS is included in the heterostructure, the wavelength range expands beyond 800 nm, confirming the contribution of infrared photons to the photocurrent. Indeed, the IPCE action spectrum practically mimics the optical density, and the APCE (absorbed photon to current efficiency) values are practically identical to IPCE, as shown in Supporting Information Figure SI6 for TiO_2/PbS/CdS. Integration of the IPCE spectrum with the wavelength led to total photocurrents of 5.7 and 4.1 mA·cm^{-2} for TiO_2/PbS/CdS and TiO_2/CdS, respectively (Figure 3b), in excellent agreement with the maximum photocurrent shown in Figure 1 (6 and 3.5 mA·cm^{-2}, respectively).

Further photoelectrochemical characterization of the heterostructured TiO_2/PbS/CdS photoanodes was carried out by impedance spectroscopy measurements in the dark and under illumination. A sound physical model was already developed for similar heterostructured materials,[19,30−32] which is given in Supporting Information Figure SI7. Consequently, this model was directly applied to extract the chemical capacitance of TiO_2, C_μ, the recombination resistance, R_{rec}, and the transport resistance, R_{tr}, of the TiO_2/PbS/CdS architectures. C_μ monitors the density of states (DOS) at the Fermi level and provides the distribution of trap states below the conduction band of TiO_2, R_{tr} is directly proportional to the resistivity of TiO_2 (ρ_{TiO2}), and R_{rec} is inversely proportional to the recombination rate of electrons at the TiO_2/solution interface.[20,33,34] The exponential behavior of the transport resistance with voltage in the QD-sensitized films follows an identical exponential trend as compared to that of bare and dye-sensitized TiO_2, suggesting that electron transport occurs mainly through the TiO_2 nanoparticles rather than through QDs.[21] Furthermore, the transport resistance (R_{tr}) for TiO_2 is very similar in the dark and under illumination (Figure 4a). This is an expected result

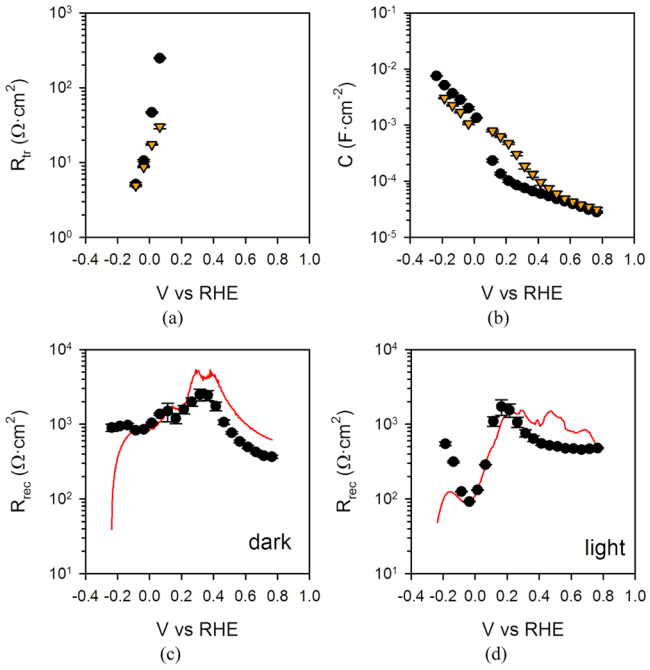

Figure 4. Parameters extracted after fitting the impedance spectroscopy spectra of the heterostructured TiO_2/PbS/CdS photoanodes using the model previously developed and shown as Supporting Information Figure SI7.[30−32] (a) Transport resistance, R_{tr}, (b) chemical capacitance, C_μ, and recombination resistance, R_{rec}, as a function of potential both (c) in the dark and (d) under illumination. The red lines in (c) and (d) represent the total resistance extracted from derivation of the $j-V$ curve, $R = (dj/dV)^{-1}$. Error bars assigned to the experimental points have been obtained from the fitting error.

because the conductivity of the TiO_2 nanoparticles is determined by the electron density in the conduction band, which is controlled by the applied potential and not by illumination. The chemical capacitance (Figure 4b) shows the characteristic exponential dependence on the potential, reflecting the trap state distribution below the conduction band of TiO_2. This agrees well with the assumption that charge is accumulated and transported mainly through the TiO_2. The behavior of C_μ is very similar in the dark and under illumination conditions, again because it is determined by the position of the Fermi level, which is governed by the applied bias. The small difference found at the intermediate states between dark and illumination conditions may be due to a capacitive contribution from the accumulation of charges in the QDs.

Finally, the recombination resistance, R_{rec}, governs the photoelectrochemical behavior of the heterostructure because the total resistance obtained by derivation of the $j-V$ curve, also including series resistances, practically mimics the R_{rec} values obtained by impedance spectroscopy both in the dark (Figure 4c) and under illumination (Figure 4d). Therefore, impedance spectroscopy appears as a very attractive experimental technique to monitor the main processes controlling the performance of these materials.

From all of the above results, TiO_2/PbS/CdS photoanodes show promising capabilities to drive solar H_2 generation. Consequently, we assembled a wireless device, resembling an artificial leaf[35,36] integrating this heterostructure, as shown in Figure 5a. The device is immersed into the aqueous solution, and upon illumination, electro−hole pairs are photogenerated in the light absorber (PbS/CdS QDs). The holes are quickly

dx.doi.org/10.1021/jz301890m | J. Phys. Chem. Lett. 2013, 4, 141−146

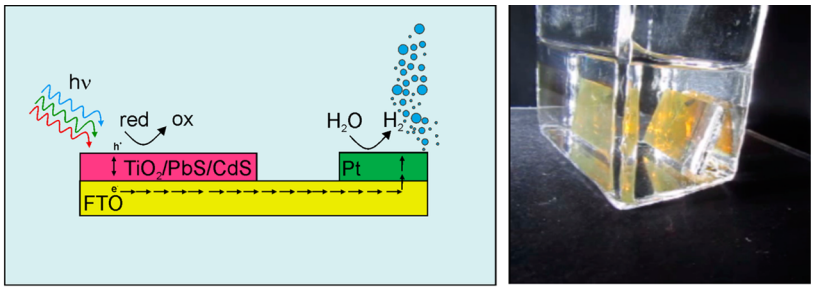

(a) (b)

Figure 5. (a) Scheme of a quasi-artificial leaf based on a heterostructured TiO_2/PbS/CdS photoanode and Pt as the cathode. (b) The TiO_2/PbS/CdS quasi-artificial leaf in a quartz cuvette filled with an aqueous 0.25 M Na_2S and 0.35 M Na_2SO_3 electrolyte evolving H_2 under illumination. A video of the PbS artificial leaf working autonomously is available in the Supporting Information audiovisual material.

injected into the solution, driving the sacrificial oxidation of SO_3^{2-}. On the other hand, photogenerated electrons are transported through the TiO_2 mesoporous structure toward the FTO substrate and then to the catalytic cathode, which is composed of a calcined chloroplatinic solution, where hydrogen can evolve. Hydrogen evolution is observed, as shown in Figure 5b and the Supporting Information audiovisual material. The hydrogen generation rate was 0.18 mL during 1 h of measurement, which equals (4.30 ± 0.25) mL·cm^{-2}·day^{-1}. It is important to highlight that at this stage, this device cannot be strictly termed "artificial leaf" because the use of a sacrificial agent is needed for operation. However, we believe that this quasi-artificial leaf constitutes a promising structure for future developments, and different optimization strategies are under investigation in our lab to improve the device efficiency, stability, and autonomy. Particularly, in order to achieve higher H_2 generation rates, morphological optimization of the TiO_2 structure is an important issue to be addressed because it has been proven that structures with lower surface area lead to better performance of QD-sensitized solar cells based on these structures.[37,38] Doping has also demonstrated enhanced TiO_2 conductivity and minimized transport losses.[14] Additionally, the presence of PbS enhances charge recombination (the lower IPCE values in the range of 350−550 nm when PbS is included in the structure is a good evidence), and efficient passivation strategies need to be developed, as previously done with colloidal PbS QDs.[39]

In summary, TiO_2/PbS/CdS heterostructures showed to be candidate architectures for solar hydrogen generation (6 mA·cm^{-2} or 60 mL·cm^{-2}·day^{-1} obtained by cyclic voltammetry in a three-electrode configuration under applied bias). Solar IR radiation provides a huge pool of photons and, consequently, of usable energy, which can be stored using the appropriate materials, such as PbS. Photocurrent and IPCE measurements have confirmed the contribution of infrared photons to the photocurrent, leading to H_2 generation. The integrated current perfectly agrees with that obtained by cyclic voltammetry, and an excellent spectral match between photocurrent and light harvesting has been obtained. Additionally, impedance spectroscopy appears as a simple and reliable characterization tool to inspect the limiting factors affecting the photoelectrochemical performance of the device. We showed that the recombination resistance (R_{rec}) controls the dynamics of the system, and further improvement of these heterostructures should be focused on strategies leading to the optimization of the TiO_2 architecture and minimization of charge recombination. Furthermore, IS analysis suggests that transport and accumulation of charge in the film mainly takes place within the TiO_2 nanoparticles. On the basis of this heterostructured material, we have developed a quasi-artificial leaf, which has proven to autonomously produce hydrogen under simulated solar illumination at (4.30 ± 0.25) mL·cm^{-2}·day^{-1}. Further developments at our lab focus on the elimination of the sacrificial agent in order to increase the robustness of the developed photoelectrodes. We believe that the present study constitutes an important milestone for the development of autonomous systems able to generate hydrogen with only the input of visible and IR radiation, combining the advances of nanotechnology and novel optoelectronic concepts.

EXPERIMENTAL METHODS

Commercial titania paste (Solarnix DSL 18NR, Switzerland, 20 nm particle size) was coated on an FTO (SnO_2/F, TEC 15) substrate by the doctor blade technique and then dried at 80 °C. Prior to TiO_2 nanoparticle deposition, the FTO substrates were covered by a compact layer of TiO_2 deposited by spray pyrolisis of titanium(IV)bis(acetoacetonato)di-(isopropanoxylate). These electrodes were subsequently sintered at 450 °C for 30 min. The thickness of the electrodes was ∼12 μm, as measured by contact profilometry. The titania electrodes were sensitized with PbS QDs grown by succesive ionic layer adsorption and reaction (SILAR).[19] For this purpose, a 0.02 M $Pb(CH_3COO)_2$ ethanolic solution was used as the Pb^{2+} source, and another one containing 0.02 M $Na_2S{\cdot}9H_2O$ in methanol/water (50/50 V/V) was used as the sulfide precursor. A single SILAR cycle consisted of 30 s dip-coating of the electrode into the lead precursor and then into the sulfide solution, also for 30 s. After each precursor bath, the photoanode was thoroughly rinsed by immersion in ethanol and dried. One cycle was sufficient for an adequate PbS sensitization.

For the hybrid PbS/CdS samples, the CdS deposition was carried out immediately after PbS deposition. For CdS SILAR deposition, 0.05 M $Cd(CH_3COO)_2$ was used as the metal precursor, and 0.02 M $Na_2S{\cdot}9H_2O$ in methanol/water (50/50 V/V) wsa used as the sulfide precursor. SILAR procedure was repeated five times. CdS coating provided effective protection of PbS from sulfide-based electrolytes and a significant enhancement of the stability. After sensitization, all of the samples were coated with ZnS by dipping alternately into 0.1 M $Zn(CH_3COO)_2$ (in water) and 0.1 M Na_2S solutions for 1 min/dip, rinsing with Milli-Q ultrapure water between dips (two cycles).[40] Reference "only CdS" samples have been

dx.doi.org/10.1021/jz301890m | J. Phys. Chem. Lett. 2013, 4, 141−146

produced, following the same steps described above, except for the deposition of PbS.

Structural inspection of the samples was carried out using a JEOL JEM-3100F field emission scanning electron microscope (SEM) and a JEOL JSM 7600F field emission transmission electron microscope (TEM). The crystallographic structure of the samples was tested by X-ray diffraction (XRD). The optical density of the photoelectrodes was recorded between 300 and 800 nm by a Cary 300 UV−vis Varian spectrophotometer.

Steady-state and chopped light current density voltages (j−V), and electrochemical impedance spectroscopy (EIS) measurements were carried out using a FRA-equipped PGSTAT-30 from Autolab. A three-electrode configuration was used, where the TiO_2/PbS/CdS photoelectrode was connected to the working electrode, a Pt wire was connected to the counterelectrode, and a saturated Ag/AgCl electrode was used as the reference. An aqueous solution containing 0.25 M Na_2S and 0.35 M Na_2SO_3 as the sacrificial hole scavenger was used as the electrolyte to prevent photocorrosion of the QDs. Nitrogen was bubbled for 30 min before testing to avoid the presence of oxygen (electron acceptor) in the solution. The pH of the solution was 13, and all of the electrochemical measurements were referred to the reversible hydrogen electrode (RHE) by the equation $V_{RHE} = V_{Ag/AgCl} + 0.197 + pH(0.059)$. The electrodes were illuminated using a 450 W Xe lamp (Oriel), where the light intensity was adjusted with a thermopile to 100 mW/cm^2, with illumination through the substrate. EIS measurements were carried out by applying a 20 mV AC signal and scanning in a frequency range between 400 kHz and 0.1 Hz, at different applied biases. The IPCE measurements were carried out by employing a 300 W Xe lamp coupled with a computer-controlled monochromator; the photoelectrode was polarized at the desired voltage with a Gamry potentiostat, and the photocurrent was measured using an optical power meter 70310 from Oriel Instruments. Labeling experiments of the evolved gases were carried out using gas chromatography mass spectroscopy, GC/MS. A quadrupole Pfeiffer Vacuum model Thermostar GSD301T with a mass interval ranging down to 300 uma was used. The evolved gas was collected in an inverted buret and extracted with a gastight syringe provided with an exit valve. The quantitative analysis of the evolved gas for the wireless device was carried out by collecting the generated gas under 100 mW·cm^{-2} illumination with an inverted buret for 1 h. The obtained result was extrapolated to 1 day. During this measurement, no addition of fresh electrolyte to the solution was carried out.

■ ASSOCIATED CONTENT

Ⓢ Supporting Information

TiO_2/CdS and TiO_2/PbS/CdS light absorption, SEM image, XRD of TiO_2/PbS electrodes, TEM micrograph, stability, IPCE versus light absorption and APCE, an impedance model, and a video of the PbS artificial leaf working autonomously. This material is available free of charge via the Internet at http://pubs.acs.org.

■ AUTHOR INFORMATION

Corresponding Author

*E-mail: sero@uji.es (I.M.-S.); sjulia@uji.es (S.G.).

Notes

The authors declare no competing financial interest.

■ ACKNOWLEDGMENTS

We acknowledge support by projects from Ministerio de Economia y Competitividad (MINECO) of Spain (Consolider HOPE CSD2007-00007, MAT2010-19827), Generalitat Valenciana (PROMETEO/2009/058 and Project ISIC/2012/008 “Institute of Nanotechnologies for Clean Energies”), and Fundació Bancaixa (P1.1B2011-50). S.G. acknowledges support by MINECO of Spain under the Ramon y Cajal programme. The SCIC of the University Jaume I de Castello is also acknowledged for the gas analysis measurements. C.S. acknowledges the POSDRU/89/1.5/S/58852 Project “Postdoctoral programme for training scientific researchers”, co-financed by the European Social Fund within the Sectorial Operational Program Human Resources Development 2007−2013. We want to acknowledge Prof. J. Bisquert for the fruitful discussions related to this manuscript.

■ REFERENCES

(1) Crabtree, G. W.; Lewis, S. N. Solar Energy Conversion. *Phys. Today* **2007**, *60*, 37−42.

(2) Walter, M. G.; Warren, E. L.; McKone, J. R.; Boettcher, S. W.; Mi, Q. X.; Santori, E. A.; Lewis, N. S. Solar Water Splitting Cells. *Chem. Rev.* **2010**, *110*, 6446−6473.

(3) Cook, T. R.; Dogutan, D. K.; Reece, S. Y.; Surendranath, Y.; Teets, T. S.; Nocera, D. G. Solar Energy Supply and Storage for the Legacy and Nonlegacy Worlds. *Chem. Rev.* **2010**, *110*, 6474−6502.

(4) van de Krol, R.; Liang, Y. Q.; Schoonman, J. Solar Hydrogen Production with Nanostructured Metal Oxides. *J. Mater. Chem.* **2008**, *18*, 2311−2320.

(5) Fujishima, A.; Honda, K. Electrochemical Photolysis of Water at a Semiconductor Electrode. *Nature* **1972**, *238*, 37−38.

(6) Tilley, S. D.; Cornuz, M.; Sivula, K.; Gratzel, M. Light-Induced Water Splitting with Hematite: Improved Nanostructure and Iridium Oxide Catalysis. *Angew. Chem., Int. Ed.* **2010**, *49*, 6405−6408.

(7) Kelzenberg, M. D.; Boettcher, S. W.; Petykiewicz, J. A.; Turner-Evans, D. B.; Putnam, M. C.; Warren, E. L.; Spurgeon, J. M.; Briggs, R. M.; Lewis, N. S.; Atwater, H. A. Enhanced Absorption and Carrier Collection in Si Wire Arrays for Photovoltaic Applications. *Nat. Mater.* **2010**, *9*, 239−244.

(8) Lin, Y. J.; Yuan, G. B.; Liu, R.; Zhou, S.; Sheehan, S. W.; Wang, D. W. Semiconductor Nanostructure-Based Photoelectrochemical Water Splitting: A Brief Review. *Chem. Phys. Lett.* **2011**, *507*, 209−215.

(9) Lin, Y. J.; Yuan, G. B.; Sheehan, S.; Zhou, S.; Wang, D. W. Hematite-Based Solar Water Splitting: Challenges and Opportunities. *Energy Environ. Sci.* **2011**, *4*, 4862−4869.

(10) Holmes, M. A.; Townsend, T. K.; Osterloh, F. E. Quantum Confinement Controlled Photocatalytic Water Splitting by Suspended CdSe Nanocrystals. *Chem. Commun.* **2012**, *48*, 371−373.

(11) Yang, S. Y.; Prendergast, D.; Neaton, J. B. Tuning Semiconductor Band Edge Energies for Solar Photocatalysis via Surface Ligand Passivation. *Nano Lett.* **2012**, *12*, 383−388.

(12) Thimsen, E.; Le Formal, F.; Gratzel, M.; Warren, S. C. Influence of Plasmonic Au Nanoparticles on the Photoactivity of Fe_2O_3 Electrodes for Water Splitting. *Nano Lett.* **2011**, *11*, 35−43.

(13) Thomann, I.; Pinaud, B. A.; Chen, Z. B.; Clemens, B. M.; Jaramillo, T. F.; Brongersma, M. L. Plasmon Enhanced Solar-to-Fuel Energy Conversion. *Nano Lett.* **2011**, *11*, 3440−3446.

(14) Hensel, J.; Wang, G. M.; Li, Y.; Zhang, J. Z. Synergistic Effect of CdSe Quantum Dot Sensitization and Nitrogen Doping of TiO_2 Nanostructures for Photoelectrochemical Solar Hydrogen Generation. *Nano Lett.* **2010**, *10*, 478−483.

(15) Chen, H. M.; Chen, C. K.; Chang, Y. C.; Tsai, C. W.; Liu, R. S.; Hu, S. F.; Chang, W. S.; Chen, K. H. Quantum Dot Monolayer Sensitized ZnO Nanowire-Array Photoelectrodes: True Efficiency for Water Splitting. *Angew. Chem., Int. Ed.* **2010**, *49*, 5966−5969.

(16) Kim, H.; Seol, M.; Lee, J.; Yong, K. Highly Efficient Photoelectrochemical Hydrogen Generation Using Hierarchical

ZnO/WO_x Nanowires Cosensitized with CdSe/CdS. *J. Phys. Chem. C* **2011**, *115*, 25429−25436.
(17) Luo, J. S.; Karuturi, S. K.; Liu, L.; Su, L. T.; Tok, A. I. Y.; Fan, H. J. Homogeneous Photosensitization of Complex TiO_2 Nanostructures for Efficient Solar Energy Conversion. *Sci. Rep.* **2012**, 2.
(18) Jin-nouchi, Y.; Hattori, T.; Sumida, Y.; Fujishima, M.; Tada, H. PbS Quantum Dot-Sensitized Photoelectrochemical Cell for Hydrogen Production from Water under Illumination of Simulated Sunlight. *ChemPhysChem* **2010**, *11*, 3592−3595.
(19) Braga, A.; Gimenez, S.; Concina, I.; Vomiero, A.; Mora-Sero, I. Panchromatic Sensitized Solar Cells Based on Metal Sulfide Quantum Dots Grown Directly on Nanostructured TiO_2 Electrodes. *J. Phys. Chem. Lett.* **2011**, *2*, 454−460.
(20) Bisquert, J. Chemical Capacitance of Nanostructured Semiconductors: Its Origin and Significance for Nanocomposite Solar Cells. *Phys. Chem. Chem. Phys.* **2003**, *5*, 5360−5364.
(21) Fabregat-Santiago, F.; Randriamahazaka, H.; Zaban, A.; Garcia-Canadas, J.; Garcia-Belmonte, G.; Bisquert, J. Chemical Capacitance of Nanoporous-Nanocrystalline TiO_2 in a Room Temperature Ionic Liquid. *Phys. Chem. Chem. Phys.* **2006**, *8*, 1827−1833.
(22) Guijarro, N.; Lana-Villarreal, T.; Mora-Sero, I.; Bisquert, J.; Gomez, R. CdSe Quantum Dot-Sensitized TiO_2 Electrodes: Effect of Quantum Dot Coverage and Mode of Attachment. *J. Phys. Chem. C* **2009**, *113*, 4208−4214.
(23) Chouhan, N.; Yeh, C. L.; Hu, S. F.; Huang, J. H.; Tsai, C. W.; Liu, R. S.; Chang, W. S.; Chen, K. H. Array of CdSe QD-Sensitized ZnO Nanorods Serves as Photoanode for Water Splitting. *J. Electrochem. Soc.* **2010**, *157*, B1430−B1433.
(24) Smotkin, E. S.; Cerveramarch, S.; Bard, A. J.; Campion, A.; Fox, M. A.; Mallouk, T.; Webber, S. E.; White, J. M. Bipolar CdSe/CoS Semiconductor Photoelectrode Arrays for Unassisted Photolytic Water Splitting. *J. Phys. Chem.* **1987**, *91*, 6−8.
(25) Fabregat-Santiago, F.; Garcia-Belmonte, G.; Mora-Sero, I.; Bisquert, J. Characterization of Nanostructured Hybrid and Organic Solar Cells by Impedance Spectroscopy. *Phys. Chem. Chem. Phys.* **2011**, *13*, 9083−9118.
(26) Haynes, W. M. *Handbook of Chemistry and Physics*, 83th ed.; CRC Press: Boca Raton, FL, 2002.
(27) Salvador, P. Kinetic Approach to the Photocurrent Transients in Water Photoelectrolysis at TiO_2 Electrodes. I. Analysis of the Ratio of the Instantaneous to Steady-State Photocurrent. *J. Phys. Chem.* **1985**, *89*, 3863−3869.
(28) Klahr, B. M.; Gimenez, S.; Fabregat-Santiago, F.; Bisquert, J.; Hamann, T. W. Electrochemical and Photoelectrochemical Investigation of Water Oxidation with Hematite Electrodes. *Energy Environ. Sci* **2012**, *5*, 7626−7636.
(29) Le Formal, F.; Gratzel, M.; Sivula, K. Controlling Photoactivity in Ultrathin Hematite Films for Solar Water-Splitting. *Adv. Funct. Mater.* **2010**, *20*, 1099−1107.
(30) Rodenas, P.; Song, T.; Sudhagar, P.; Marzari, G.; Han, H.; Badía-Bou, L.; Gimenez, S.; Fabregat-Santiago, F.; Mora-Sero, I.; Bisquert, J. Quantum Dot Based Heterostructures for Unassisted Photoelectrochemical Hydrogen Generation. *Adv. Energy Mater.* **2012**, DOI: 10.1002/aenm.201200255.
(31) Gonzalez-Pedro, V.; Xu, X. Q.; Mora-Sero, I.; Bisquert, J. Modeling High-Efficiency Quantum Dot Sensitized Solar Cells. *ACS Nano* **2010**, *4*, 5783−5790.
(32) Mora-Sero, I.; Gimenez, S.; Fabregat-Santiago, F.; Gomez, R.; Shen, Q.; Toyoda, T.; Bisquert, J. Recombination in Quantum Dot Sensitized Solar Cells. *Acc. Chem. Res.* **2009**, *42*, 1848−1857.
(33) Bisquert, J. Theory of the Impedance of Electron Diffusion and Recombination in a Thin Layer. *J. Phys. Chem. B* **2002**, *106*, 325−333.
(34) Bisquert, J.; Cahen, D.; Hodes, G.; Ruhle, S.; Zaban, A. Physical Chemical Principles of Photovoltaic Conversion with Nanoparticulate, Mesoporous Dye-Sensitized Solar Cells. *J. Phys. Chem. B* **2004**, *108*, 8106−8118.
(35) Nocera, D. G. The Artificial Leaf. *Acc. Chem. Res.* **2012**, *45*, 767−776.
(36) Reece, S. Y.; Hamel, J. A.; Sung, K.; Jarvi, T. D.; Esswein, A. J.; Pijpers, J. J. H.; Nocera, D. G. Wireless Solar Water Splitting Using Silicon-Based Semiconductors and Earth-Abundant Catalysts. *Science* **2011**, *334*, 645−648.
(37) Samadpour, M.; Gimenez, S.; Iraji Zad, A.; Taghavinia, N.; Calvo, M.; Miguez, H.; Mora-Sero, I. Effect of the Architecture of TiO_2 and QDs Deposition Strategy on the Photovoltaic Performance of Quantum Dot Sensitized Solar Cells. *Electrochim. Acta* **2012**, *75*, 139−147.
(38) Sudhagar, P.; Song, T.; Lee, D. H.; Mora-Seró, I.; Bisquert, J.; Laudenslager, M.; Sigmund, W. M.; Park, W. I.; Paik, U.; Kang, Y. S. High Open Circuit Voltage Quantum Dot Sensitized Solar Cells Manufactured with ZnO Nanowire Arrays and Si/ZnO Branched Hierarchical Structures. *J. Phys. Chem. Lett.* **2011**, *2*, 1984−1990.
(39) Tang, J.; Kemp, K. W.; Hoogland, S.; Jeong, K. S.; Liu, H.; Levina, L.; Furukawa, M.; Wang, X. H.; Debnath, R.; Cha, D. K.; et al. Colloidal-Quantum-Dot Photovoltaics Using Atomic-Ligand Passivation. *Nat. Mater.* **2011**, *10*, 765−771.
(40) Shen, Q.; Kobayashi, J.; Diguna, L. J.; Toyoda, T. Effect of ZnS Coating on the Photovoltaic Properties of CdSe Quantum Dot-Sensitized Solar Cells. *J. Appl. Phys.* **2008**, 103.